

## Development of Transport Properties Characterization Capabilities for Thermoelectric Materials and Modules

Karla R. Reyes-Gil, Josh Whaley, Ryan Nishimoto, and Nancy Yang  
Sandia National Laboratories, 7011 East Ave, Livermore, CA 94551

### ABSTRACT

Thermoelectric (TE) generators have very important applications, such as emerging automotive waste heat recovery and cooling applications. However, reliable transport properties characterization techniques are needed in order to scale-up module production and thermoelectric generator design. DOE round-robin testing found that literature values for figure of merit (ZT) are sometimes not reproducible in part for the lack of standardization of transport properties measurements. In Sandia National Laboratories (SNL), we have been optimizing transport properties measurements techniques of TE materials and modules. We have been using commercial and custom-built instruments to analyze the performance of TE materials and modules. We developed a reliable procedure to measure thermal conductivity, seebeck coefficient and resistivity of TE materials to calculate the ZT as function of temperature. We use NIST standards to validate our procedures and measure multiple samples of each specific material to establish consistency. Using these developed thermoelectric capabilities, we studied transport properties of  $\text{Bi}_2\text{Te}_3$  based alloys thermal aged up to 2 years. Parallel with analytical and microscopy studies, we correlated transport properties changes with chemical changes. Also, we have developed a resistance mapping setup to measure the contact resistance of Au contacts on TE materials and TE modules as a whole in a non-destructive way. Recently, a major effort has been conducted to investigate chemical/structural stability and output power of TE materials under representative conditions (temperature gradient and current flow). The development of novel but reliable characterization techniques has been fundamental to better understand TE materials as function of aging time, temperature and environmental conditions. All this information is crucial for the development of long-term reliable and stable TE modules for multiple applications.

### INTRODUCTION

Within the last century, solid-state thermoelectric materials have been developed that are capable of converting heat directly into electrical energy. One such material,  $\text{Bi}_2\text{Te}_3$ , is a doped semiconductor originally developed in the 1950's to replace the compressor based refrigeration system.<sup>1</sup> Bismuth Telluride ( $\text{Bi}_2\text{Te}_3$ ) has the highest ZT for T between 25 °C and 150 °C when compared to other materials (Figure 1).<sup>2</sup> Thermoelectric materials, such as  $\text{Bi}_2\text{Te}_3$  alloys, generate useful electrical energy when a temperature gradient is applied inducing net migration of charge across the gradient. Directly converting thermal energy into electricity can come with an array of benefits in comparison to more commonly used energy generation methods, such as the Rankine cycle or Co-generation cycle. These benefits can include decreased environmental impact through the reduction of carbon emissions, greater reliability due to minimal moving parts, and the ability to generate electricity from heat that may have otherwise been wasted (such as automotive waste heat recovery). However, standardization of measurements of thermoelectric materials properties is needed in order to scale-up module production and thermoelectric generator design. DOE round-robin testing found that the overall errors for figure of merit (ZT) are from  $\pm 12$  to 21%. In Sandia National Laboratories, we have been developed in-house measurement capabilities for thermoelectric characterization. In this paper, we focus on the capability development and

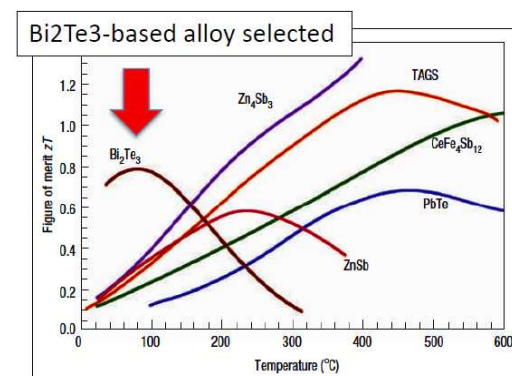


Figure 1: Figure of merit (ZT), plotted against temperature for a variety of TE materials.

standardization of the transport properties measurements. Only selected examples of the thermal aging studies were discussed for brevity.

## CAPABILITIES DEVELOPMENT

### A. Figure of Merit (ZT)

If thermoelectrics are to be seriously considered in the production of power, it is important that the efficiency of the material to convert heat be fully characterized. The Figure of Merit is commonly used to quantify how efficient a thermoelectric material is at converting heat into electrical energy and has units of inverse temperature. Z is the Figure of Merit, S is the Seebeck Coefficient,  $\kappa$  is thermal conductivity, and  $\rho$  is electrical resistivity.

$$Z = \frac{S^2}{\kappa * \rho}$$

The product of the Figure of Merit and Temperature, ZT, is a dimensionless quantity used in the assessment of thermoelectric material. The efficiency of a thermoelectric,  $\eta$ , can be defined in terms of the Figure of Merit <sup>3,4</sup>

$$\eta = \eta_{carnot} * \frac{\sqrt{ZT_{ave}+1}-1}{\sqrt{ZT_{ave}+1}+\frac{T_c}{T_h}} \text{, where } \eta_{carnot} = 1 - \frac{T_c}{T_h}$$

where  $T_{ave}$  is the average of  $T_h$  and  $T_c$ . The Carnot efficiency,  $\eta_{carnot}$ , is the maximum efficiency achievable for a heat engine running between two temperature reservoirs. To aid in the design and application of thermoelectric material, our group has developed the capability to calculate ZT over a wide range of temperatures using a combination of commercial devices as well as instrumentation developed in-house.

### B. Seebeck Coefficient and Electrical Resistivity Measurements

A custom built in-house device was developed at Sandia to measure the Seebeck coefficient and electrical resistivity of thermoelectric materials. These instruments use a pair of Nickel heaters to sandwich a thermoelectric sample and provide temperature control. Control software for the instruments was created in-house using LabVIEW and has the capability to measure Seebeck coefficient and electrical resistivity with respect to temperature and time. After the desired temperature or temperature gradient has been reached either a four probe electrical resistivity measurement or simple voltage measurement is performed to determine the electrical resistivity or Seebeck, respectively. The temperature stabilizes to within 0.1°C for 300 seconds and it is assumed that the thermoelectric sample is in isothermal equilibrium with the heaters. Figure 2 illustrates the set-up used to measure the electrical resistivity. A current is sent through the Nickel heaters using a Keithley 6221 current source. Ten electrical resistance measurements are then performed in series and an averaged value is calculated and recorded at that set point. With a known current being sent through the material, a four probe measurement is conducted using two additional surface probes connected to a Keithley 2182A nano-voltmeter, which is in sync with the current source. The electrical resistivity can then be calculated using the equation on Figure 2, in which  $\Delta V$  is the voltage measurement,  $A_{cs}$  is the cross-sectional area of the sample,  $I$  is the current, and  $L$  is the probe separation distance. Once the measurement is completed, a relay system physically disconnects the vessel from the Keithley instruments and proceeds to connect a vessel to the Seebeck coefficient measurement instrumentation.

When determining the efficiency of a thermoelectric material, accurately measuring the Seebeck coefficient is extremely important in preventing error because of the squared dependency. The Seebeck coefficient, also known as thermopower, is defined in equation in Figure 2, where  $\Delta V$  is the voltage across the sample and  $\Delta T$  is the temperature gradient across the sample. Once the gradient is achieved and sufficient time has passed, 300 seconds, 10 voltage measurements are taken. This process is then repeated with temperature gradients of various magnitudes and in the opposite direction. For our current experiments, temperature gradients of +/- 1°C, +/- 2°C, and +/- 3°C are utilized. Once this step is

completed, a least mean square linear curve fit is then performed on the collected data and a Seebeck coefficient is recorded as the slope of the fitted line. The  $R^2$  value of this data must be monitored to ensure a linear fit is justified. To get the true Seebeck coefficient of the thermoelectric material, the Seebeck effects from the chromel wiring must be removed from the measured values using thermocouple tables for Type KP.

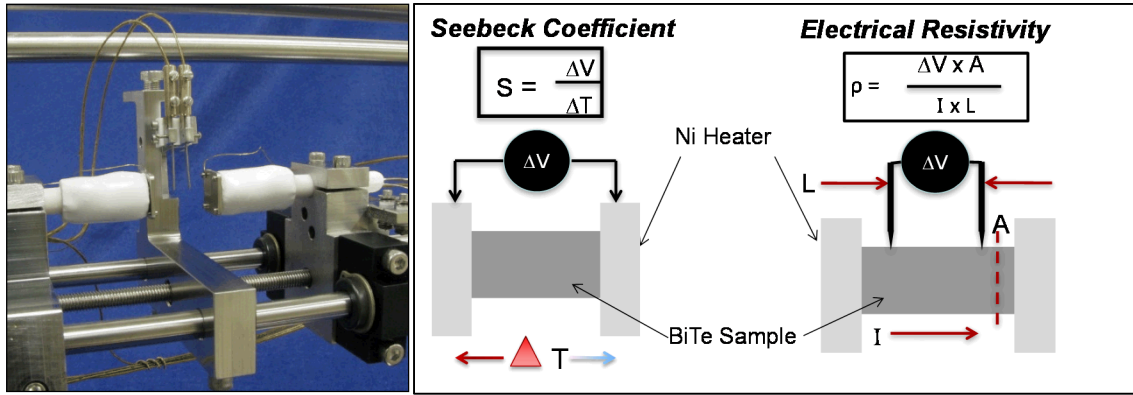


**Figure 2:** (Left) Photo of Seebeck coefficient/electrical resistivity measurement device. (Right) System configuration while measuring Seebeck coefficient and electrical resistivity. For seebeck coefficient, a temperature (T) gradient is set up across the material and the voltage (V) recorded. For electrical resistivity, two voltage probes in contact with the top surface and a known current (I) is then sent through the material and a voltage (V) recorded.

Recently, a major effort has been conducted to investigate thermal stability and output power of TE materials under representative conditions (temperature gradient and current flow). We had modified the seebeck coefficient measurement setup in order to allow both high currents and high temperature gradients to be applied to the sample. The hot side was 250°C and the cold side was 90°C and current was applied to the sample. Output voltage, internal resistance and open circuit were monitored. Experiments as long as 1 month have been conducted to analyze how the thermopower changes as function of time.

### C. Thermal Conductivity Measurements

Once Seebeck and resistivity data are collected, it is then combined with data from the commercially available ThermTest, Inc. TPS2500 and used to calculate ZT for various materials. One of the most precise and convenient techniques for studying thermal transport properties is the

Transient Plane Source (TPS) method. The Hot Disk Thermal Analyser utilizes a sensor, which consists of an electrically conducting pattern in the shape of a double spiral, which has been etched out of a thin metal (Nickel) foil (Figure 3). This spiral is sandwiched between two thin sheets of an insulating material (Kapton). When performing a thermal transport measurement, the plane Hot Disk sensor is fitted between two pieces of the  $\text{BiTe}_3$  tiles each one with a plane surface facing the sensor. By passing an electrical current, high enough to increase the temperature of the sensor several degrees, and at the same time recording the resistance (temperature) increase as a function of time, the Hot Disk sensor is used both as a heat source and as a dynamic temperature sensor.

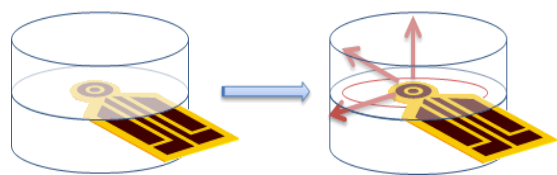


**Figure 3:** (a) Hot Disk Sensor is placed between two pieces of sample and (b) passes an electrical current. [Figures were modified from Hot Disk Instruction Manual]

The raw data is a temperature increase versus time graph. After the point selection, the software calculates the thermal conductivity, thermal diffusivity and specific heat. The thermal conductivity is calculated using the slope of time-dependent temperature plot is given as:

$$\Delta T_{ave}(\tau) = \frac{P_0}{\frac{3}{\pi^2 \cdot \alpha \cdot k}} \cdot D(\tau)$$

where  $P_0$  is the total output of power from the sensor,  $\alpha$  is the radius if the disk,  $\kappa$  is the thermal conductivity of the sample that is being tested and  $D(\tau)$  is a dimensionless time dependent function.

#### D. Contact Resistant Measurements

In a thermoelectric device, p- and n-doped  $\text{Bi}_2\text{Te}_3$  elements are connected thermally in parallel and electrically in series using metal contacts. In actual thermoelectric power generating modules, the Figure of Merit must be modified to take into account internal losses due to non-zero contact resistances at the two interfaces at each thermoelectric element. Thus, the efficiency of an actual module must be calculated using the effective Figure of Merit given by,

$$Z_{eff} = Z \cdot \left( \frac{1}{1 + \frac{2R_c}{R}} \right)$$

Where  $R_c$  is the contact resistance and  $R$  is the bulk resistance of a thermoelectric element. Now the efficiency of the device becomes,

$$\eta = \frac{T_h - T_c}{T_h} * \frac{\sqrt{Z_{eff} T_{ave} + 1} - 1}{\sqrt{Z_{eff} T_{ave} + 1} + \frac{T_c}{T_h}}$$

We designed and built an instrument to measure both the contact resistance and the bulk resistivity at room temperature. The system is based on a device reported by Mengali and Seiler<sup>5</sup> and modified by Liao et al.<sup>6</sup> In our instrument, current is injected across two faces of the thermoelectric sample while the voltage is measured at several points on the top face of the sample referenced to one of the faces through which current is injected. When the samples are metallized, current is injected through the metallized faces. A measurement will produce a plot of resistance versus position. The position of each resistance measurement is calculated by taking and analyzing a micrograph that shows the location of each multiprobe lead with respect to the guarded voltage sensor. Taking into account the geometry of the sample, the slope of the resistance versus position yields the bulk resistivity of the sample and the intercept of the plot yields the specific contact resistance.

Figure 4 shows the evolution of the contact resistance setup. The original setup was exclusively designed for tiles of a fixed size. To analyze TE legs with high aspect ratio, a new setup was built with adjustable mini-probes for size flexibility. Recently, the setup was modified to allow the testing of individual legs in a TE module in a non-destructive way. Front and rear cameras were added to allow 3D probes adjustments.

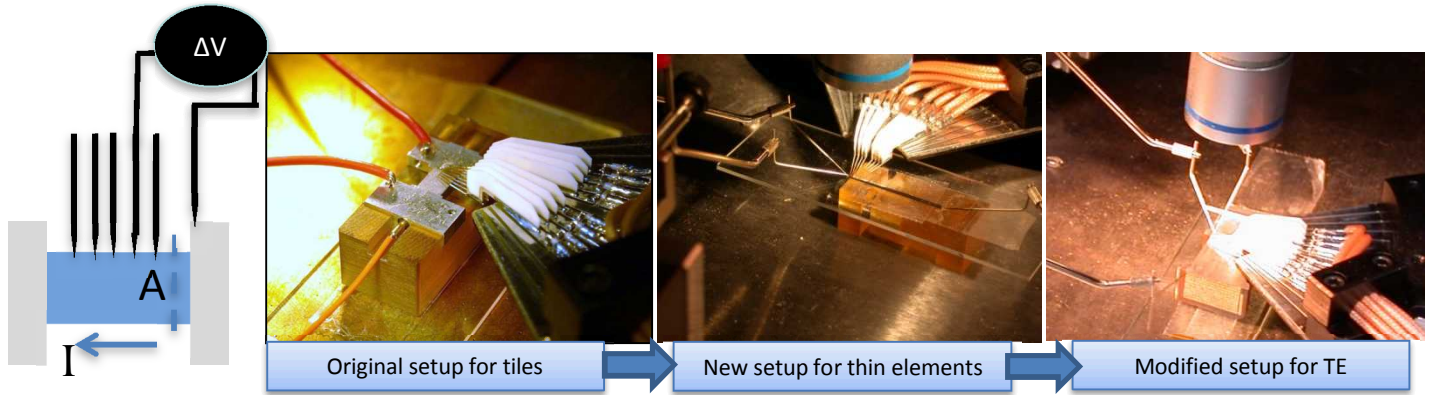


Figure 4: A thermoelectric sample is mounted such that current is injected through the metallized ends and the voltage is measured along several points on the top of the sample referenced to one of the metallized ends. Photographs of hardware used to map the resistance of thermoelectric samples and modules.

## RESULTS AND DISCUSSION

### A. Standardization-

IEA-AMT round-robin testing highlighted need of standardization of measurements of thermoelectric materials properties. Low-temperature seebeck coefficient standard (3451) was obtained from National Institute of Standard & Technology (NITS). As shown in Figure 5, the seebeck values obtained at SNL differed from the NITS official results by approximately 1%. As no official values are available for resistivity and thermal conductivity, NIST standards were used as internal reference. Several standards were measured and the variation coefficient was less than 1% for both measurements.

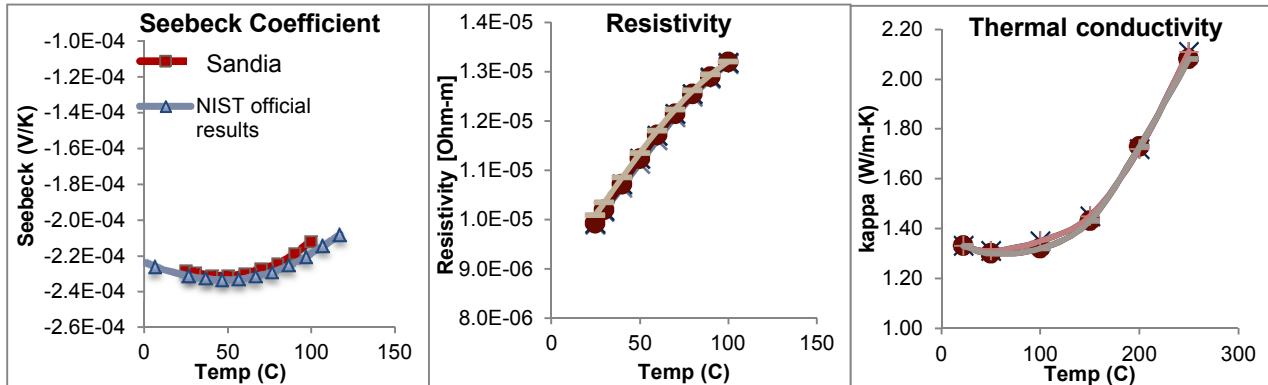


Figure 5: Seebeck coefficient, resistivity and thermal conductivity of NIST  $\text{Bi}_2\text{Te}_3$  standard. The official results for seebeck coefficient were included in the left plot for comparison purposes.

### B. Thermal Aging Studies

At SNL, we have an extensive thermal aging program. As example, we selected the study of phase vapor deposited (PVD) Au and electroplated Au on  $\text{Bi}_2\text{Te}_3$  tiles. As shown the cross sectional SEM images (Figure 6), thin PVD coating (300-400 nm) is well bonded but the Au coverage is poor, while thick PVD coating (10-15  $\mu\text{m}$ ) has full coverage but interface separation. The electrodeposited Au looks well bonded with full Au coverage. After 6 months of isothermal aging at 240°C, the PVD Au showed discoloration from the (Bi, Te) oxidation, while the electrodeposited Au did not show any oxidation.

### C. Transport Properties

The seebeck coefficient, resistivity and thermal conductivity were measured for n-type and p-type  $\text{Bi}_2\text{Te}_3$  tiles as received and isothermal aged at 240°C for 2 wk, 8wk, 6mo, 1yr and 2yr. Figure 5 shows

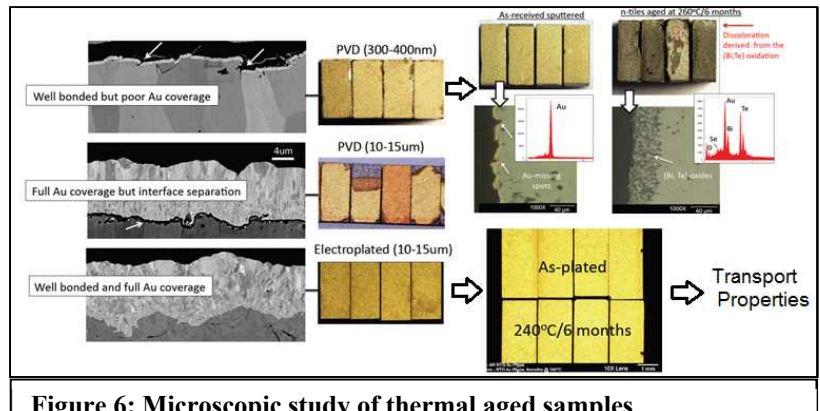


Figure 6: Microscopic study of thermal aged samples

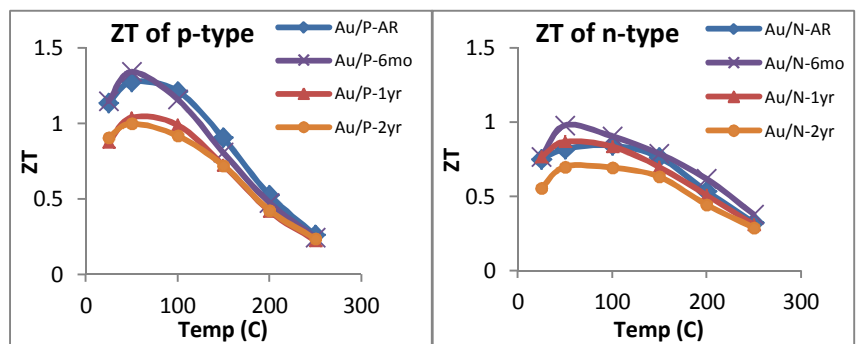


Figure 5: ZT of p-type and n-type  $\text{Bi}_2\text{Te}_3$  tiles aged up to 2 years.

the ZT calculated as function of temperature. For both p and n-type, ZT decreases as function of aging time, showing around 20% reduction after 2 year. The data showed that increasing in electrical resistivity is the major contributor of the reduction of the ZT. The root causes of the resistivity changes are under investigation using microscopy and analytical techniques.

#### D. Resistance Mapping of TE modules

In addition to measure contact resistance of tiles and thin legs, we can measure the contact resistance of individual legs of the module in a non-destructive way. Figure 6 shows the resistance as function of the distance of the probe relative to the Au contact. The y-intercept of all the lines approaches to zero, which means that the contact resistance of electrodeposited Au coatings is minimal. P-type and n-type legs showed a slightly difference slope than n-type indicating a higher resistivity. As received and aged legs showed similar response indicating no significant change on resistivity or contact resistance due to aging.

## CONCLUSIONS

International Round-Robin study found that significant measurements issues and 12-21% differences on ZT values. Sandia has dedicated several years on the development of reliable and reproducible in-house thermoelectric characterization capabilities. The developed capabilities have been used for thermal aging studies up to 2yr to determine how the performance of the bulk material and metallization changes with aging. Advanced instrumentation makes possible the non-destructive analysis of thermoelectric modules. The developed capabilities have been used beyond thermoelectric for internal and external collaborations with industry and universities to study thermal barriers, insulation and phase change materials.

## REFERENCES

- 1) A. Mujumdar, Science 303, 777 (2004)
- 2) G.J. Snyder; M. Christensen; E. Nishibori; T. Caillat; B.B. Iversen, "Disordered Zinc in Zn<sub>4</sub>Sb<sub>3</sub> with Phonon-Glass and Electron-Crystal Thermoelectric Properties", Nature Materials, 3, no.7, p.458-63 (2004).
- 3) G. Jeffery Snyder and Tristan S. Ursell. Thermoelectric Efficiency and Compatibility. The American Physical Society Vol. 91 Number 14. 2003
- 4) Rowe, D.M., Thermoelectrics Handbook: Macro to Nano, pp. 1.3-1.5, Taylor and Francis, New York, 2006.
- 5) O.J. Mengali, M.R. Seiler, Advanced Energy Conversion, vol. 2, 59-68, 1962.
- 6) C.N. Liao, C.H. Lee, W.J. Chen, Electrochemical and Solid State Letters, vol 10, 23-25, 2007.

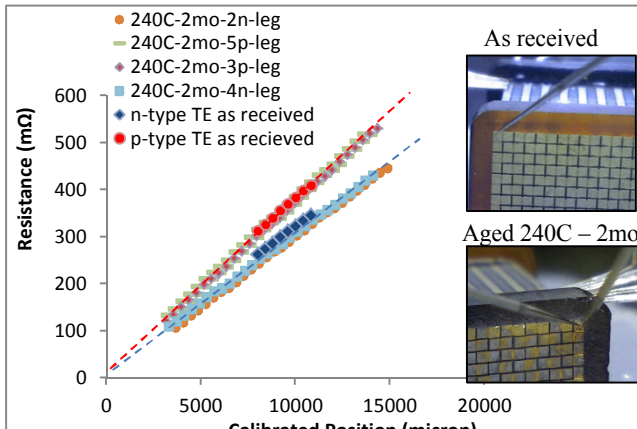


Figure 6: Resistance mapping of as received and aged TE modules